IEEE Access
Multidisciplinary | Rapid Review | Open Access Journal

SPECIAL SECTION ON PHYSICAL AND MEDIUM ACCESS CONTROL LAYER ADVANCES IN 5G WIRELESS NETWORKS

Received March 24, 2017, accepted April 26, 2017, date of publication May 19, 2017, date of current version August 29, 2017.

Digital Object Identifier 10.1109/ACCESS.2017.2700078

Peak-to-Average Power Ratio Reduction of FBMC/OQAM Signal Using a Joint Optimization Scheme

JUNHUI ZHAO[1,2], (Senior Member, IEEE), SHANJIN NI[1], AND YI GONG[3], (Senior Member, IEEE)

[1]School of Electronic and Information Engineering, Beijing Jiaotong University, Beijing 100044, China
[2]School of Information Engineering, East China Jiaotong University, Nanchang 330013, China
[3]Department of Electrical and Electronic Engineering, South University of Science and Technology of China, Shenzhen 518055, China

Corresponding author: Junhui Zhao (junhuizhao@bjtu.edu.cn)

This work was supported in part by the National Natural Science Foundation of China under Grant 61471031 and Grant 61661021, in part by the National Science and Technology Major Project of the Ministry of Science and Technology of China under Grant 2016ZX03001014-006, in part by the Open Research Fund of National Mobile Communications Research Laboratory, Southeast University under Grant 2017D14, in part by the State Key Laboratory of Rail Traffic Control and Safety, Beijing Jiaotong University under Contract RCS2017K009, in part by the Fundamental Research Funds for the Central Universities under Grant 2017YJS022, and in part by the Shenzhen Peacock Program under Grant KQJSCX20160226193545.

ABSTRACT Owing to the signal structure difference between the filter bank multicarrier with offset quadrature amplitude modulation (FBMC/OQAM) and the orthogonal frequency-division multiplexing (OFDM) systems, the existing technologies to reduce the peak-to-average power ratio (PAPR) for OFDM systems are not suitable for the FBMC/OQAM systems. This paper considers the problem of PAPR in the FBMC/OQAM systems, and to reduce the PAPR of the FBMC/OQAM signal, we propose an improved joint optimization scheme combined with the linear (i.e., partial transmit sequence (PTS)) and nonlinear (i.e., clipping and filtering (CF)) methods, named improved bilayer partial transmit sequence and iterative clipping and filtering (IBPTS-ICF) scheme. The main idea of this joint optimization scheme is clipping and filtering the processed FBMC/OQAM signal, whose probability of the peak value has been reduced by the IBPTS technique. Meanwhile, aided by the knowledge of convex optimization, the IBPTS-ICF joint optimization scheme can effectively reduce the signal distortion. The excellent PAPR reduction performance of the proposed scheme has been confirmed in our simulations.

INDEX TERMS FBMC/OQAM, bilayer PTS, clipping and filtering, PAPR reduction, joint optimization.

I. INTRODUCTION

Attributable to its capability to efficiently cope with frequency selective channels, multicarrier modulation (MCM) has become the key physical layer transmission technology adopted in wireless communications. As one of the most prominent MCM techniques, Orthogonal Frequency Division Multiplexing (OFDM) has been widely used in the present broadband multicarrier communications, including digital television and audio broadcasting, wireless networks, powerline networks, and the Fourth-Generation (4G) wireless communications. By dividing the total bandwidth into many narrow subchannels, OFDM offers a considerably high spectral efficiency and multi-path delay spread tolerance. However, the adoption of OFDM in the Fifth-Generation (5G) cellular networks is not taken for granted [1]. OFDM also presents some limitations. More precisely, the insertion of redundant cyclic prefixes (CPs) in OFDM implies a reduction of spectral efficiency, and the use of rectangular pulse shape on each subcarrier leads to high out-of-band radiation [2].

OFDM is not exempt of defects, and it may be an undesirable solution in many future communication systems. As one of the most credited alternatives to OFDM, Filter Bank Multicarrier with Offset Quadrature Amplitude Modulation (FBMC/OQAM) has recently attracted an increasing amount of attention, particularly in multiple access and cognitive radio networks [3], [4]. Compared with the conventional OFDM, the use of FBMC/OQAM for 5G cellular networks is mainly recommended for the ability to avoid distortion from asynchronous signals in adjacent bands. Furthermore, without the need of a guard interval (GI) or CP, FBMC/OQAM has the potential of achieving higher spectral efficiency of transmission. And FBMC/OQAM requires orthogonality for

the neighbouring subchannels only, and can be designed with arbitrarily small side lobes [5]–[7].

Similar to the OFDM systems, some challenging issues still remain unresolved in the design of FBMC/OQAM systems. One of the major drawbacks is the high Peak-to-Average Power Ratio (PAPR) of the transmitted signal.The high PAPR may result in significant distortion when traveling through a nonlinear device, such as a transmit power amplifier. Moreover, the high PAPR may have a detrimental effect on battery lifetime in mobile applications and outweigh all the potential benefits of FBMC/OQAM systems [8]. Therefore, in order to utilize the technical features of FBMC/OQAM, it is important and necessary to focus on how to reduce the PAPR.

A number of approaches have been proposed to deal with the PAPR problem in OFDM systems. Considering the similarity between the OFDM and FBMC/OQAM systems, it is natural to research how to employ the PAPR reduction schemes for OFDM systems to reduce the PAPR of FBMC/OQAM signal [9]. Over the past few decades, various PAPR reduction schemes for OFDM systems have been proposed. The techniques included clipping [10], [11], coding [12]–[15], nonlinear companding transforms [16]–[18], active constellation extension (ACE) [19], [20], tone reservation (TR) [21], partial transmit sequences (PTS) [22]–[26], and selected mapping (SLM) [27], [28]. However, owing to the overlapping of adjacent data blocks, the conventional PAPR reduction techniques cannot be directly applied to FBMC/OQAM systems. Some improved PAPR reduction schemes for FBMC/OQAM systems have been proposed on the foundation of these OFDM PAPR reduction schemes. Qu *et al.* [9] proposed an improved PTS scheme by employing multi-block joint optimization (MBJO) for the PAPR reduction of the FBMC/OQAM signal. Although the improved MBJO-PTS scheme provided good results, the complexity of utilizing a trellis diagram for the MBJO-PTS optimization problem would increase computational complexity, and might make the MBJO-PTS scheme infeasible in practice. Kollár *et al.* [29] presented a clipping based PAPR reduction scheme to reduce the PAPR of FBMC signal. By employing sliding window for the PAPR reduction of FBMC/OQAM signal, an improved TR technique was proposed in [30]. While the PAPR was reduced by the proposed TR technique without additional complexity, it costed the reduced data rate since the additional peak reduction tones (PRTs) were required.

In this paper, we propose an improved bilayer PTS and iterative clipping and filtering (IBPTS-ICF) joint optimization scheme to reduce the PAPR of FBMC/OQAM signal. The main contributions of this paper are listed as follow:

1) Unlike the existing conventional PAPR reduction schemes of OFDM system, this paper exploits the overlapping structure of the FBMC/OQAM signal, and the iterative clipping and filtering (ICF) algorithm to minimize distortion is proposed after the improved bilayer PTS (IBPTS) processing.
2) Compared with the conventional PTS algorithm, the penalty factors and bilayer structure are introduced into the IBPTS algorithm, and the computational complexity can be significantly reduced. In order to further reduce the PAPR of FBMC/OQAM signal, the optimal ICF algorithm is presented. Considering the in-band signal distortion caused by the clipping method, filtering and iterative compensation are introduced into the ICF algorithm.
3) The accuracy of the analytical results is demonstrated through numerical simulation. The proposed IBPTS-ICF scheme has a remarkable PAPR reduction performance than the conventional PTS and clipping methods.

The rest of this paper is organized as follows. Section II describes the FBMC/OQAM modulation. In Section III, the IBPTS-ICF joint optimization scheme is proposed. Section IV presents simulated results for characterizing the proposed PAPR reduction scheme. Finally, conclusions are drawn in Section V.

Notations : we use bold font variables to denote matrices and vectors. $(\cdot)^T$ denotes the transpose, and $\|\cdot\|_2$ denotes the two-norm. $E[\cdot]$ denotes the expectation operator, and $j = \sqrt{-1}$.

II. FBMC/OQAM MODULATION

Fig. 1 illustrates the FBMC/OQAM transmitter structure, which consists of N subcarriers. In the transmitter, a serial-to-parallel (S/P) converter is introduced at the output of the QAM symbol S_m, and the complex input symbol is written as:

$$s_m^n = a_m^n + jb_m^n, \tag{1}$$

with $S_m = [s_m^0, s_m^1, \cdots, s_m^{N-1}]^T$, $0 \leqslant n \leqslant N-1$, and $0 \leqslant m \leqslant M-1$, where M represents the number of data blocks. a_m^n and b_m^n are the real and imaginary parts of the m^{th} symbol on the n^{th} subcarrier, respectively. Attributable to the complex input symbols of the FBMC/OQAM system can be assumed statistically independent and identically distributed (i.i.d.), a_m^n and b_m^n are uncorrelated with each other. In the following, the i.i.d. Gaussian random variables of a_m^n and b_m^n are assumed. The real and imaginary parts of each symbol are then transmitted on a subcarrier, respectively. A specially designed prototype filter is applied

$$s[k] = \sum_{q=-\infty}^{\infty} \sum_{n=0}^{N-1} \left(\theta_n a_q^n h[k - qN] + \theta_{n+1} b_q^n h\left[k - qN - \frac{N}{2}\right] \right) \times e^{jn(k-qN)\frac{2\pi}{N}} \tag{2}$$

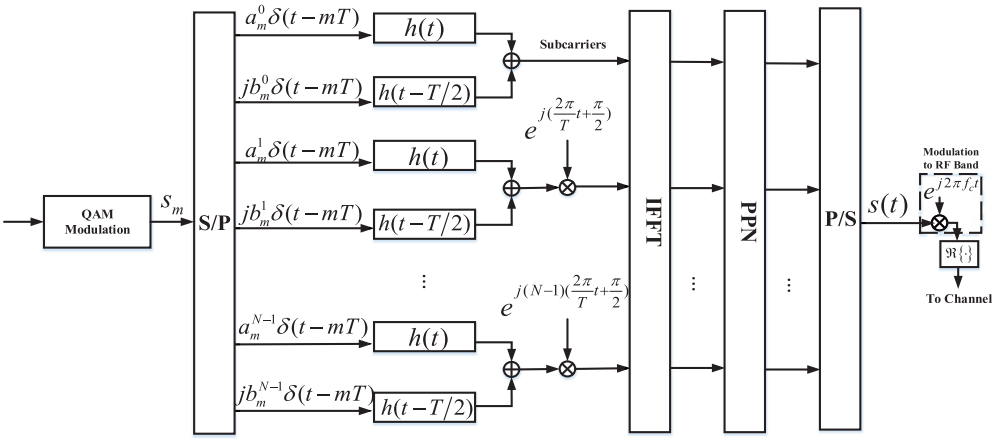

FIGURE 1. A block diagram of FBMC/OQAM transmitter.

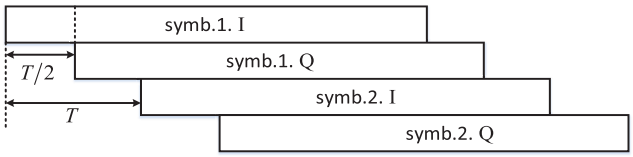

FIGURE 2. The structure of FBMC/OQAM signal [31].

for each subcarrier, and the prototype filter fulfils the Nyquist property [6].

The real and imaginary parts of the OQAM symbols are staggered with a time offset of half a symbol duration (i.e., $T/2$, T is the symbol period). The structure of FBMC/OQAM signal is shown in Fig. 2. With the objective to reduce the computational complexity, after the prototype filter and phase modulation, the OQAM symbols are processed by the inverse fast fourier transform (IFFT) and polyphase network (PPN) [7].

The modulated signal for the FBMC/OQAM transmitter at sample k is given by (2) shown at the bottom of the previous page, where

$$\theta_n = \begin{cases} 1, & \text{if } n \text{ is even;} \\ j, & \text{if } n \text{ is odd.} \end{cases} \tag{3}$$

$h[k]$ is the prototype filter, and the PHYDYAS prototype filter is adopted in this paper [6]. Due to the advantageous properties of the prototype filter, an FBMC signal will have a better adjacent channel leakage ratio (ACLR) than an OFDM signal [10].

In practice, it is not straightforward to measure the PAPR for the continuous-time baseband signal, and most of the existing PAPR reduction schemes are implemented for the discrete-time baseband signal. However, the PAPR for the discrete-time baseband signal $s[k]$ may not be the same as that for the continuous-time baseband signal [8]. In order to approximate the true PAPR of the FBMC/OQAM signal, the $s(t)$ is β-times oversampled where $\beta \geqslant 4$ [32].

Attributable to the overlapping structure of FBMC, we define a frame containing M overlapping FBMC data blocks. The length of the frame is $\left(M+\beta-\frac{1}{2}\right)N$, and the length of each block is $\left(\beta+\frac{1}{2}\right)N$. The PAPR of a frame containing M data blocks can therefore be defined with $s[k]$ in dB as [33]:

$$\mathrm{PAPR}(\mathbf{s}_f)_{\mathrm{dB}} = 10\log_{10}\left(\frac{\max\limits_{0\leqslant k\leqslant\left(M+\beta-\frac{1}{2}\right)N-1}\left|\{\mathbf{s}_f\}_k\right|^2}{E\left[\left|\mathbf{s}_f\right|^2\right]}\right) \tag{4}$$

where $\mathbf{s}_f = \left[s[0],\cdots,s\left[\left(M+\beta-\frac{1}{2}\right)N-1\right]\right]^T$.

III. PROPOSED IBPTS-ICF JOINT OPTIMIZATION SCHEME FOR THE PAPR REDUCTION OF FBMC/OQAM SIGNAL

A. CONVENTIONAL PTS TECHNIQUE

In the conventional PTS technique for OFDM systems, the input data block $\mathbf{S}$ is partitioned into V disjoint subblocks $\mathbf{S}^v$, and $v = 1, 2, \cdots, V$. The discrete-time domain signal can then be written as:

$$\mathbf{S} = \left[\mathbf{S}^0, \mathbf{S}^1, \cdots, \mathbf{S}^v, \cdots, \mathbf{S}^V\right]^T, \tag{5}$$

where $\mathbf{S}^v$ are consecutively located and also are of equal size.

The subcarriers in each subblock are independently rotated by phase factors, and the phase factors are selected to combine the partial transmit sequences to minimize the PAPR. The set of the phase factors as a vector is $\mathbf{b} = \left\{b^v = e^{j2\pi l/W} \,\middle|\, l = 0, 1, \cdots, W-1\right\}$ and W is the number of allowed phase factors. In order to reduce the search complexity, the selection of the phase factors is limited to a set with finite number of elements.

As shown in Fig. 2, based on the overlapping nature of FBMC/OQAM signals, it is obvious that the m^{th} data block overlaps with the next $\beta - 1$ data blocks. Applying the

conventional PTS technique for the FBMC/OQAM system, block S_m is divided into V subblocks. Let $s_m^v[k]$ denote the discrete-time domain sequences of the v^{th} subblock, then $s_m^v[k]$ is given by [9]:

$$s_m^v[k] = \left(s_m^{v,0}[k], s_m^{v,1}[k], \cdots, s_m^{v,n}[k], \cdots, s_m^{v,N-1}[k]\right), \quad (6)$$

where $s_m^{v,n}[k] = s_m^n[k]$, if n^{th} symbol belongs to subblock v.

The signal of subblock v can be denoted as:

$$s_m^v[k] = \sum_{n=0}^{N-1} s_m^{v,n}[k]. \quad (7)$$

Therefore, the discrete-time domain signal of the m^{th} data block with phase factor vector b_m^v is given by:

$$s_m[k] = \sum_{v=1}^{V} b_m^v s_m^v[k]. \quad (8)$$

By choosing the optimal phase vector, the PAPR can be minimized, which is expressed as follows:

$$\left[\tilde{b}_m^1, \cdots, \tilde{b}_m^V\right] = \arg \min_{[b_m^1, \cdots, b_m^V]} \left(\max_{(m-1)N \leqslant k \leqslant (\beta+m-\frac{1}{2})N-1} \left| \sum_{v=1}^{V} b_m^v s_m^v[k] \right| \right). \quad (9)$$

Thus the corresponding discrete-time domain signal with the lowest PAPR can be represented as [34]:

$$\tilde{s}_m[k] = \sum_{v=1}^{V} \tilde{b}_m^v s_m^v[k]. \quad (10)$$

In the conventional PTS scheme, the phase rotation operation is only used for the current data block. However, due to the overlapping structure of FBMC/OQAM signal, the optimization performance achieved by the conventional PTS scheme will be debased.

B. CONVENTIONAL CLIPPING TECHNIQUE

The simplest way to reduce the PAPR of an FBMC/OQAM signal may be clipping [35]. However, because nonlinear effects are introduced, and clipping may cause significant in-band signal distortion, resulting in BER performance degradation, and out-of-band interference, reducing the spectral efficiency.

A predefined threshold $A_{\max}$ limits the peak envelope of the discrete-time domain FBMC/OQAM signal. That is:

$$s_m^c[k] = \begin{cases} s_m[k], & \text{if } |s_m[k]| \leqslant A_{\max} \\ A_{\max} e^{j\varphi(s_m[k])}, & \text{if } |s_m[k]| > A_{\max}, \end{cases} \quad (11)$$

where $\varphi(s_m[k])$ is the phase of $s_m[k]$. The most important parameter, which affects the system performance, is characterized by the clipping ratio (CR) γ denoted as:

$$\gamma = \frac{A_{\max}}{\sigma}, \quad (12)$$

where σ is the root mean square (RMS) power of the FBMC/OQAM signal.

The distortion caused by amplitude clipping can be viewed as another source of noise, named clipping noise. And the clipped signal can be expressed as:

$$s_m^c[k] = \varepsilon s_m[k] + d_m[k], \quad 0 \leqslant k \leqslant K, \quad (13)$$

where $d_m[k]$ is the clipping noise, which is uncorrelated with $s_m[k]$ [36]. Moreover, the attenuation factor ε is a function of the clipping ratio γ, which is given by [10]:

$$\varepsilon = 1 - e^{-\gamma^2} + \frac{\sqrt{\pi}}{2}\gamma \operatorname{erfc}(\gamma). \quad (14)$$

Therefore, the clipped signal at the n^{th} subcarrier after the K-point discrete fourier transform (DFT) is written as follows:

$$\begin{aligned} \tilde{\mathbf{S}}_n &= \frac{1}{\sqrt{K}} \sum_{k=0}^{K-1} s_m^c[k] e^{-j2\pi(n/K)k} \\ &= \varepsilon \underbrace{\frac{1}{\sqrt{K}} \sum_{k=0}^{K-1} s_m[k] e^{-j2\pi(n/K)k}}_{S_m^n} \\ &\quad + \underbrace{\frac{1}{\sqrt{K}} \sum_{k=0}^{K-1} d_m[k] e^{-j2\pi(n/K)k}}_{D_m^n}, \end{aligned} \quad (15)$$

where D_m^n denotes the complex nonlinear distortion term falling on the n^{th} subcarrier. According to the central limit theorem, as the number of subcarriers increases, the D_m^n approaches Gaussian random variables with a zero mean.

The performance of the clipping algorithm is measured by the signal-to-distortion ratio (SDR), and the SDR of the n^{th} subcarrier is given by:

$$\mathrm{SDR}_n = \frac{\varepsilon^2 E\left[|S_m^n|^2\right]}{E\left[|D_m^n|^2\right]}. \quad (16)$$

C. IBPTS-ICF JOINT OPTIMIZATION SCHEME

For the PAPR reduction of FBMC/OQAM signal, we propose an IBPTS-ICF joint optimization scheme. The block diagram of IBPTS-ICF algorithm is shown in Fig. 3. The joint optimization scheme exploits the overlapping structure of FBMC/OQAM signal and aims to reduce overlapping effect. The main ideas of the proposed IBPTS-ICF scheme are listed as follows:

- by utilizing the IBPTS algorithm to reduce the search complexity of conventional PTS algorithm. In the IBPTS algorithm, the bilayer structure is introduced and the weighting phase factors are constrained to a finite range. To further reduce the computational complexity, we then propose a simplified and suboptimal IBPTS algorithm where the penalty factors is introduced. Although the system performance is slightly affected, the computational complexity is greatly reduced.

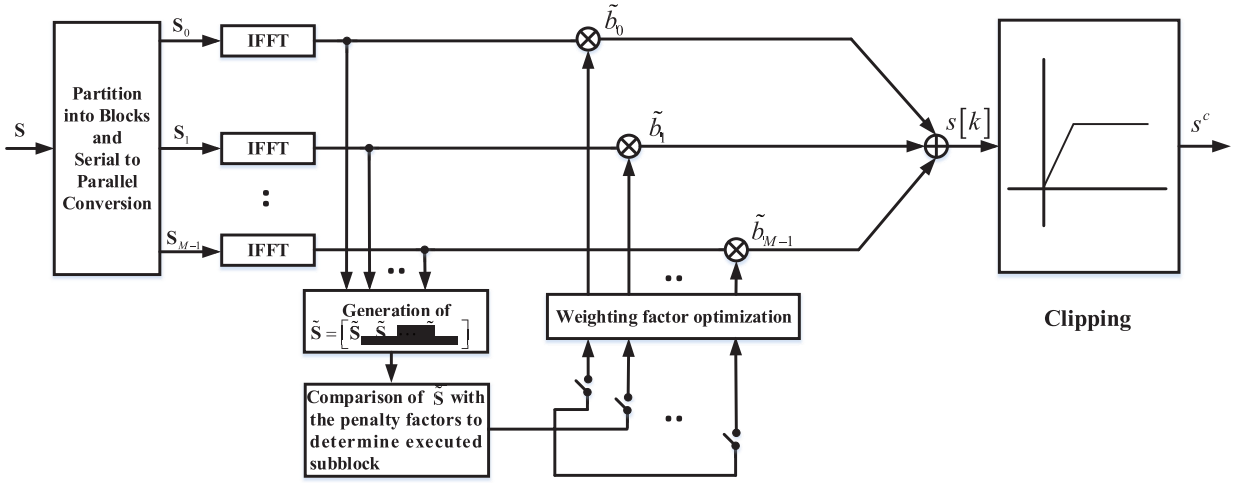

FIGURE 3. Block diagram of the IBPTS-ICF algorithm.

- by using the optimal ICF algorithm to restore the performance of FBMC/OQAM signal. The proposed ICF algorithm aims to further reduce the PAPR. However, the clipping technique can cause clipping noise which falls both in-band and out-of-band. In order to improve the performance and counter the effects of clipping, filtering after clipping is introduced. However, filtering can only reduce out of band radiation after clipping, and it is unable to reduce in-band distortion. Therefore, the iterative compensation strategy is applied to solve this problem.
- by combining the best of IBPTS and ICF algorithms to minimize the PAPR.

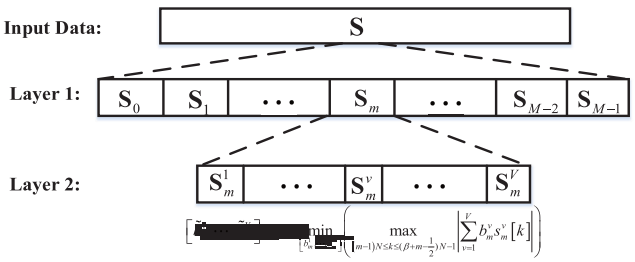

FIGURE 4. Structure of the improved bilayer PTS algorithm.

In the PTS process, the frame containing M overlapping FBMC data blocks noted by S_m, and $0 \leqslant m \leqslant M-1$. Applying the adjacent partition method, data block S_m is divided into V subblocks, that is:

$$S_m = \sum_{v=1}^{V} S_m^v. \tag{17}$$

As shown in Fig. 4, the optimal vector of phase factors $\mathbf{b}_m = \left[\tilde{b}_m^1, \cdots, \tilde{b}_m^v, \cdots, \tilde{b}_m^V\right]$ then combines with the V subblocks. According to (10), the optimization problem of the FBMC/OQAM system could be written as:

$$\min_{\mathbf{b}_m} \left\{ \max_k |\tilde{s}_m[k]|^2 \right\} \tag{18a}$$

$$\text{s.t. } \tilde{s}_m[k] = \sum_{v=1}^{V} \tilde{b}_m^v s_m^v[k] \tag{18b}$$

$$b_m^v = \left\{ e^{j2\pi l/W} \middle| \, l = 0, 1, \cdots, W-1 \right\} \tag{18c}$$

$$1 \leqslant v \leqslant V \tag{18d}$$

$$0 \leqslant n \leqslant N-1 \tag{18e}$$

For the optimization problem of PTS scheme, the computational complexity consists of three parts [24]:

i) Overlapping factor β;
ii) Weighting phase factors $\tilde{\mathbf{b}}_m$;
iii) PAPR computation and the number of data blocks M.

For part i), the overlapping factor β is suggested to be 4, the PAPR of the sampled signals can then approximate to the true PAPR of the continous-time signal very well. So the computational complexity in ii) and iii) is mainly considered. In order to reduce the search complexity of the PTS algorithm, a simplified and suboptimal PTS algorithm is proposed at the cost of system performance. Firstly, the weighting phase factors $\tilde{\mathbf{b}}_m$ are constrained to $\{-1, 1\}$ with $W = 2$ for all v and m, and the computational complexity has a significant reduction. Sequently, the penalty factors μ_p and ω_p are then introduced for finding the suboptimal solution $\mathbf{b}_m^*$ of (18).

Like the conventional clipping algorithm, the IBPTS algorithm also introduces a ***special threshold***, named penalty factors. The introduction of penalty factors is for reducing the number of candidate data blocks which need to be searched, and the computational complexity is then reduced. Different from the threshold which can cause the distortion of FBMC signal in clipping algorithm, the penalty factors will not cause

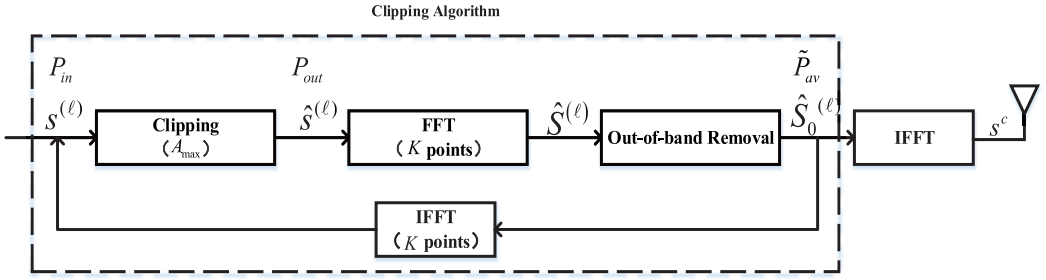

FIGURE 5. Structure of the clipping algorithm after PTS process.

any distortion. Let

$$\mu_p = \frac{1}{\sqrt{2}} \max_k \{|s[k]|\}. \tag{19}$$

It is assumed that ξ is the number of $|s_m[k]| \geqslant \mu_p$ with $(m-1)N \leqslant k \leqslant (\beta + m - \frac{1}{2})N - 1$ in the m^{th} data block $\mathbf{S}_m$, which can be expressed as:

$$\xi = \text{num}\left(|s_m[k]| \geqslant \mu_p \,\middle|\, (m-1)N \leqslant k \leqslant (\beta + m - \frac{1}{2})N - 1\right). \tag{20}$$

Once $\xi \geqslant \omega_p$ or

$$\max_k \left\{|s_m[k]|^2\right\} \geqslant \frac{1}{\sqrt{2}} \max_k \left\{|s[k]|^2\right\} \tag{21}$$

holds in the m^{th} data block, we will ***punish*** this data block, and the phase factors search method in **Algorithm 1** is executed; otherwise, the subblock $\mathbf{S}_m^v$ performs no action.

Algorithm 1 The Phase Factors Search Algorithm

1: Set $\tilde{\mathbf{b}}_m = [1, 1, \cdots, 1]$ and $index = 1$, and compute the PAPR of the combined signal, named PAPR_0;
2: **while** $index < V + 1$ **do**
3: $\quad\tilde{\mathbf{b}}_m[index] = -1$;
4: $\quad$Recompute the PAPR, named PAPR_{index};
5: $\quad$**if** $\text{PAPR}_{index} \leqslant \text{PAPR}_0$ **then**
6: $\quad\quad$Retain $\tilde{\mathbf{b}}_m[index]$ as part of the final set of phase factors;
7: $\quad$**else**
8: $\quad\quad\tilde{\mathbf{b}}_m[index] = 1$;
9: $\quad$**end if**
10: $\quad index = index + 1$;
11: **end while**

After the suboptimal PTS algorithm, we obtain the suboptimal signal, and let $s[k]$ denote the suboptimal signal. As shown in Fig. 5, clipping is directly used to the processed FBMC/OQAM signal $s[k]$. According to (16), in order to reduce nonlinear effects of clipping, the clipping problem can be formulated as follows:

$$\max_{D^{(\ell)} \in \mathbb{C}^N} \mathbf{SDR}^{(\ell)} = \frac{\varepsilon^2 E\left[\left|S^{(\ell)}\right|^2\right]}{E\left[\left|D^{(\ell)}\right|^2\right]} \tag{22a}$$

$$s.t.\ \hat{S}_0^{(\ell)} = \hat{S}^{(\ell)} \cdot H \tag{22b}$$

$$s^{(\ell+1)} = IFFT\left(\hat{S}_0^{(\ell)}\right)_K \tag{22c}$$

$$d^{(\ell+1)} = \hat{s}^{(\ell)} - \varepsilon s^{(\ell+1)} \tag{22d}$$

$$d^{(\ell+1)} = IFFT\left(D^{(\ell+1)}\right)_K \tag{22e}$$

$$\frac{\left\|\hat{s}^{(\ell)}\right\|_\infty}{\left\|\hat{s}^{(\ell)}\right\|_2/\sqrt{K}} \leqslant \gamma \tag{22f}$$

where $\ell = 1, 2, \cdots$ denotes the iteration number, and H is the filter for removing the out-of-band spectral, which can be written as follows:

$$H(i) = \begin{cases} 1, & 1 \leqslant i \leqslant N \\ 0, & N+1 \leqslant i \leqslant K. \end{cases} \tag{23}$$

The problem (22) is a non-convex problem; owing to the inequality constraint (22f) is non-convex. However, the optimization problem (22) can be transformed into a convex problem by a transformation of the objective and inequality constraint functions.

According to (11), the non-convex (22f) can be transformed to a convex constraint:

$$\left\|\hat{s}^{(\ell)}\right\|_\infty \leqslant A_{\max}^{(\ell)}. \tag{24}$$

Moreover, according to (12), the threshold $A_{\max}$ can be expressed as follows:

$$\begin{aligned} A_{\max}^{(\ell)} &= \sigma^{(\ell)} \cdot \gamma \\ &= \frac{1}{\sqrt{K}} \left\|\hat{s}^{(\ell)}\right\|_2 \cdot \gamma. \end{aligned} \tag{25}$$

Then according to (24) and (25), we have:

$$\left\|s^{(\ell+1)}\right\|_2 \leqslant \left\|\hat{s}^{(\ell)}\right\|_2. \tag{26}$$

With the substitution of (25) and (26) into (22), we can express the optimization problem (22) in the form:

$$\min_{t \in R} \ t \tag{27a}$$

$$s.t.\ \sigma^{(\ell)} = \frac{1}{\sqrt{K}} \left\|s^{(\ell)}\right\|_2 \tag{27b}$$

$$A_{\max}^{(\ell)} = \sigma^{(\ell)} \cdot \gamma \tag{27c}$$

$$\hat{S}_0^{(\ell)} = \hat{S}^{(\ell)} \cdot H \tag{27d}$$

$$s^{(\ell+1)} = IFFT\left(\hat{S}_0^{(\ell)}\right)_K \tag{27e}$$
$$d^{(\ell+1)} = \hat{s}^{(\ell)} - \varepsilon s^{(\ell+1)} \tag{27f}$$
$$D^{(\ell+1)} = FFT\left(d^{(\ell+1)}\right)_K \tag{27g}$$
$$S^{(\ell+1)} = FFT\left(s^{(\ell+1)}\right)_K \tag{27h}$$
$$\left\|D^{(\ell+1)}\right\|_2 \leqslant \varepsilon \left\|S^{(\ell+1)}\right\|_2 t \tag{27i}$$
$$\left\|s^{(\ell+1)}\right\|_2 \leqslant \left\|\hat{s}^{(\ell)}\right\|_2 \tag{27j}$$

With these modifications, the optimization problem (27) can be formulated as a special type of convex optimization problem known as second-order cone program (SOCP) and efficiently calculated by using the standard interior-point methods.

D. BIT ERROR RATE OF THE CLIPPING WITHOUT CHANNEL CODING

In this subsection, the bit error rate (BER) of the clipping signal without channel coding are analysed. As shown in Fig. 5, let $P_{in} = \sigma^2$ be the input power, and the output power P_{out} can be expressed as [37]:

$$P_{out} = \left(1 - e^{-\gamma^2}\right) P_{in}. \tag{28}$$

Furthermore, after the clipping process, the effective output signal power P_t can be expressed as follows:

$$P_t = \varepsilon^2 E\left[\|s\|^2\right] = \varepsilon^2 P_{in} = K_\gamma P_{out}. \tag{29}$$

Then according to (28), we have:

$$K_\gamma = \frac{\varepsilon^2}{1 - e^{-\gamma^2}}, \tag{30}$$

where K_γ is a normalized attenuation factor.

According to (13) and (15), the signal-to-noise-plus-distortion ratio (SNDR) is given by:

$$\text{SNDR} = \frac{\varepsilon^2 E\left[\|s\|^2\right]}{E\left[\|d\|^2\right] + E\left[\|w\|^2\right]}, \tag{31}$$

where w is the additive white Gaussian noise (AWGN) component with zero-mean and variance σ_W^2. Additionally,

$$E\left[\|d\|^2\right] = P_{out} - P_t. \tag{32}$$

Then the SNDR can be rewritten as follows:

$$\begin{aligned}\text{SNDR} &= \frac{\varepsilon^2 P_{in}}{(P_{out} - P_t) + \sigma_W^2} \\ &= \frac{K_\gamma P_{out}}{\left(1 - K_\gamma\right) P_{out} + \sigma_W^2}.\end{aligned} \tag{33}$$

As mentioned before, the distortion term can be seen as Gaussian for large N, then after clipping, the BER of κ-ary square quadrature amplitude modulation (κQAM) in the case of an AWGN channel can be expressed as follows [38]:

$$\text{BER}_{\kappa\text{QAM}}^{\text{AWGN}} = \frac{2\left(\sqrt{\kappa} - 1\right)}{\sqrt{\kappa}\log_2(\kappa)} \text{erfc}\left[\sqrt{\frac{3\log_2(\kappa)}{2(\kappa - 1)} \cdot \text{SNDR}}\right]. \tag{34}$$

Without loss of generality, we assume that x_n is the i.i.d. random variable with zero-mean and variance $\sigma^2 = E\left[|x_n|^2\right]$. For the κQAM/FBMC signal,

$$x_n = A\left[(2m_1 - 1) + j(2m_2 - 1)\right], \tag{35}$$

where A is a constant of the normalized statistical average power P, and $A > 0$, $m_1, m_2 \in \left\{-\frac{\kappa}{2} + 1, \cdots, \frac{\kappa}{2}\right\}$ ($\kappa > 2$). Then the upper and lower bounds of the κQAM-FBMC signal can be represented as:

$$\frac{3}{\kappa^2 - 1} \leqslant \text{PAPR}_{\kappa\text{QAM - FBMC}} \leqslant \frac{3N(\kappa - 1)}{\kappa + 1}. \tag{36}$$

According to (36), we can obtain that the upper bound of PAPR is proportional to the number of subcarriers N for large κ.

E. COMPLEXITY ANALYSIS

For the IBPTS algorithm, the computational complexity depends on the selection of penalty factors μ_p and ω_p. The computational complexity is $\mathcal{O}\left(MW^V\right)$ in the worst case. For the ICF algorithm, the cost of solving the SOCP problem in (27) is $\mathcal{O}\left(N^3\right)$ in the worst case [39]. Furthermore, the extra fast fourier transform (FFT) or IFFT pair with $\mathcal{O}\left(K\log_2 K\right)$ complexity needs to be performed in each iteration. With the maximum iteration number Γ, the computational complexity of the clipping algorithm is $\mathcal{O}\left(N^3 + 3\Gamma K\log_2 K\right)$. For this reason, the complexity of the IBPTS-ICF joint optimization scheme is $\mathcal{O}\left(MW^V + N^3 + 3\Gamma K\log_2 K\right)$ in the worst case.

Compared with the conventional clipping method, after the clipping and filtering operations, the iterative compensation strategy is applied in the proposed ICF algorithm, and the the signal distortion can be effectively reduced. Although the computational complexity $\mathcal{O}\left(N^3\right)$ is introduced in the process of solving the optimization problem, it should be noted that the computational complexity $\mathcal{O}\left(N^3\right)$ is the complexity upper bound for solving the SOCP optimization problem (27). Designing a customized interior-point method for problem (27) can significantly reduce the computational complexity [40].

IV. NUMERICAL RESULTS

In this section, simulation results are conducted to investigate the PAPR reduction performance of the proposed IBPTS-ICF joint optimization scheme in case of FBMC/OQAM signal. The number of the subcarriers N is set to 128 and 4 QAM modulation is adopted for the FBMC/OQAM system. The oversampling factor is $\beta = 4$, and the number of candidate phases for a subblock is $W = 2$.

In the conventional PTS technique, the known subblock partitioning methods can be classified into three categories: pseudo-random partition, interleaved partition and adjacent partition [41]. Fig. 6 displays the complementary cumulative distribution function (CCDF) comparison of different PTS partition methods with $V = 4$ in the FBMC/OQAM system. It shows the system performance of pseudo-random partition

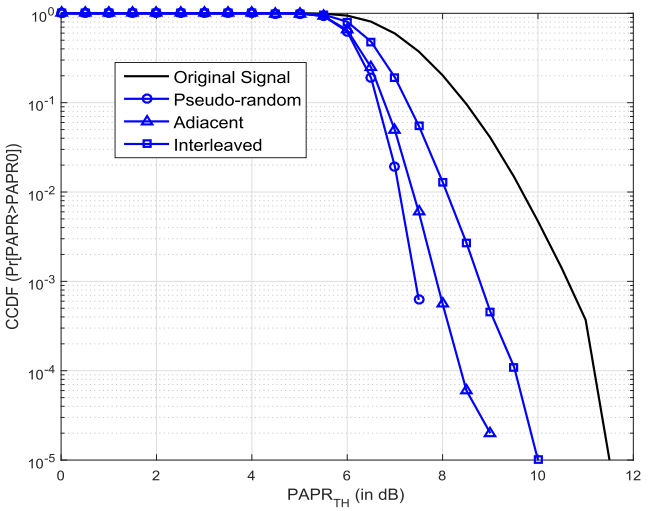

FIGURE 6. Comparison of different subblock partitioning methods in FBMC/OQAM system, $V = 4$.

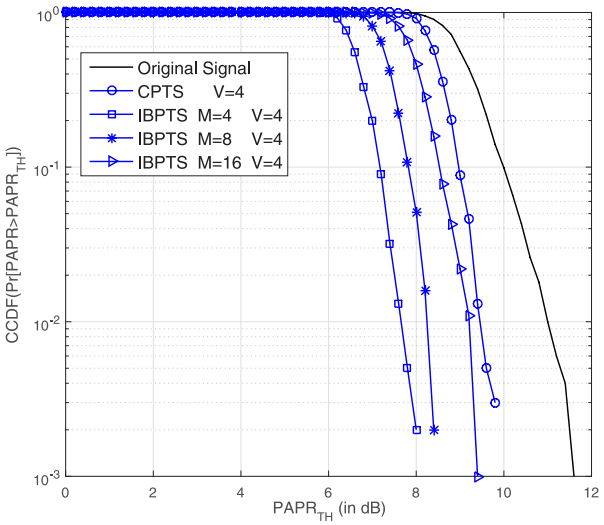

FIGURE 7. CCDFs of the FBMC/OQAM signal with the IBPTS algorithm, $\omega_p = 2$ and $V = 4$.

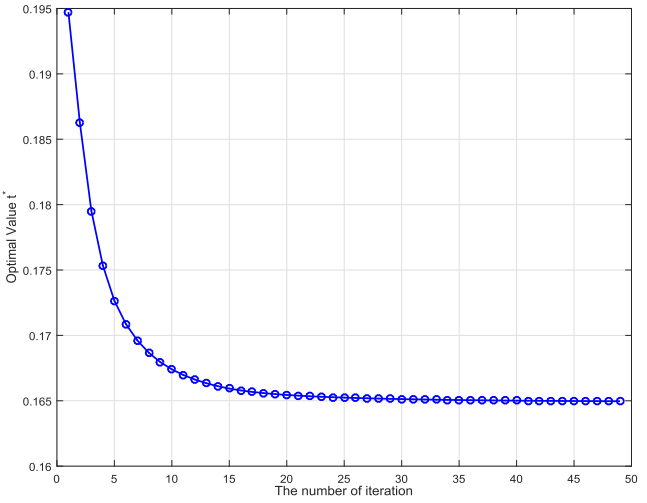

FIGURE 8. The optimal value t^* versus the number of iteration, $\gamma = 1.2$.

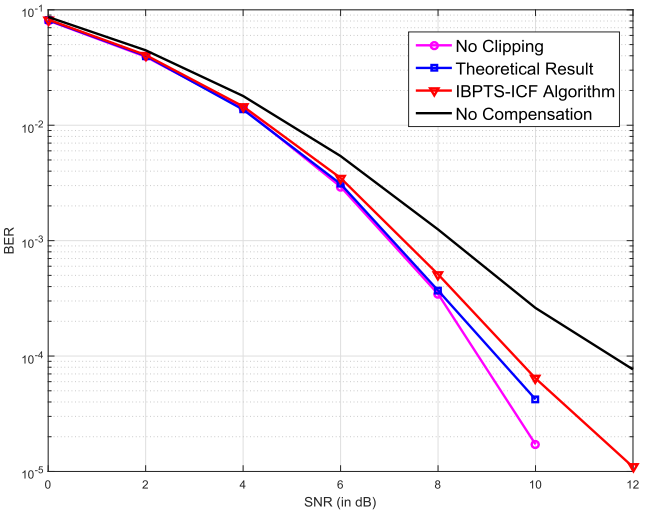

FIGURE 9. BER performance with the IBPTS-ICF joint optimization scheme.

method is obviously more superior to the other two methods. However, the pseudo-random partition method has some uncertainty and variability, leading to instability or unacceptable system performance.

Fig. 7 plots the relationship of CCDF and PAPR with varying numbers of subblocks M after the IBPTS processing in the IBPTS-ICF joint optimization scheme. Due to the uncertainty and variability of the pseudo-random partition method, the adjacent partition method is selected for the IBPTS-ICF joint optimization scheme based on the simulation results of Fig. 6. The plot has been generated with the penalty factor $\omega_p = 2$, and the number of the subblocks $V = 4$ in the m^{th} subblock. Compared with the conventional PTS (CPTS) algorithm, the IBPTS processing with different M in the proposed scheme can effectively reduce the PAPR of the FBMC/OQAM signal. Moreover, with the increasing number of subblocks M, the effectiveness of reducing the PAPR has an evident degradation.

The SOCP (27) has a global optimal solution t^*, and global optimality ensures that any other solution satisfying the constraints of (27) must have $t > t^*$. The optimal value t^* versus the number of iteration with the clipping ratio $\gamma = 1.2$ is illustrated in Fig. 8. We can clearly observe that the optimal value t^* converges to a global optimum solution with increasing iterations. In order to reduce the computational complexity of the proposed scheme, the number of iteration $\Gamma = 5$ is chosen in the follow-up simulations.

In Fig. 9, we show the BER performance of the proposed scheme with clipping ratio $\gamma = 1.2$ in the AWGN channel. It can be observed that the clipping method can heavily degrade the overall system performance if it is not compensated. With 5 iterative compensation, the proposed ICF algorithm can efficiently improve the system performance.

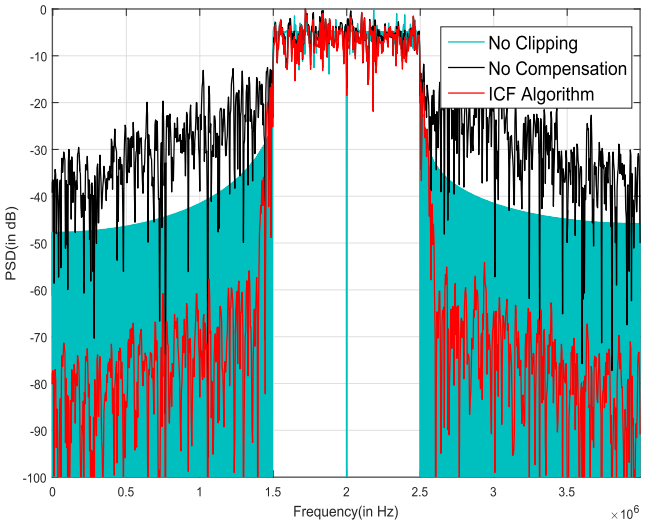

FIGURE 10. Power spectral density effects of the proposed IBPTS-ICF scheme.

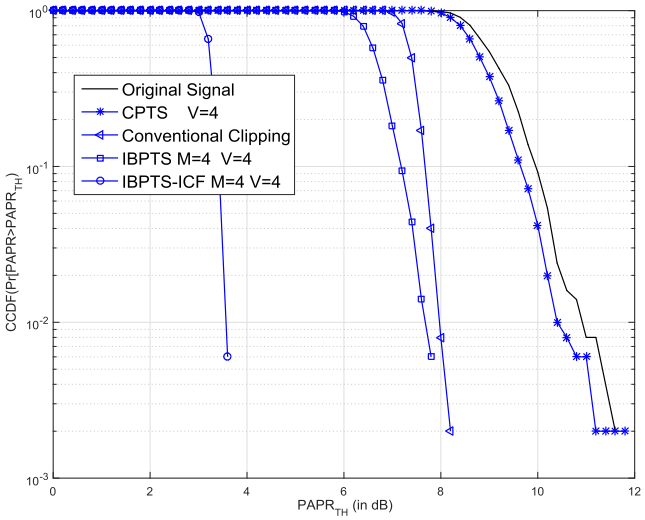

FIGURE 11. CCDFs of the FBMC/OQAM signal with the IBPTS-ICF joint optimization scheme, $V = 4$.

The comparison of PSD with clipping ratio $\gamma = 1.2$ is shown in Fig. 10. It is clear that, the clipped signal without iterative compensation contains high out-of-band component, and the processed signals by the proposed ICF algorithm have much lower out-of-band radiation than the conventional clipping method. For example, the average out-of-band radiation reaches $-90dB$ at the frequency 0 MHz, while that of the conventional clipping method reaches $-45dB$.

Fig. 11 shows the CCDF of the PAPR, and four different PAPR reduction schemes (i.e. the CPTS algorithm, the conventional Clipping algorithm, the IBPTS algorithm, and the IBPTS-ICF joint optimization scheme) are compared. The clipping ratio $\gamma = 1.2$, the penalty factor $\omega_p = 2$, $M = 4$, and $V = 4$. As can be revealed in Fig. 11, the IBPTS-ICF joint optimization scheme significantly outperforms the CPTS scheme and the conventional clipping scheme. What is worth mentioning is that the IBPTS-ICF joint optimization scheme can effectively decrease the signal distortion by the introduction of the penalty factors μ_p and ω_p, as well as the ICF algorithm. Therefore, the IBPTS-ICF joint optimization scheme is more suitable for the requirements of the PAPR reduction when compared to other schemes.

V. CONCLUSION

In this paper, an IBPTS-ICF joint optimization scheme has been proposed for the PAPR reduction of the FBMC/OQAM system. Using the IBPTS and the ICF algorithms, the PAPR reduction performance of the FBMC/OQAM system has a remarkable improvement. Conducted simulation results show that an FBMC/OQAM system with the IBPTS-ICF joint optimization scheme is able to perform better in PAPR reduction than the other conventional schemes.

REFERENCES

[1] P. Banelli, S. Buzzi, G. Colavolpe, A. Modenini, F. Rusek, and A. Ugolini, "Modulation formats and waveforms for 5G networks: Who will be the heir of OFDM? An overview of alternative modulation schemes for improved spectral efficiency," *IEEE Signal Process. Mag.*, vol. 31, no. 6, pp. 80–93, Nov. 2014.

[2] T. Ihalainen, A. Ikhlef, J. Louveaux, and M. Renfors, "Channel equalization for multi-antenna FBMC/OQAM receivers," *Trans. Veh. Technol.*, vol. 60, no. 5, pp. 2070–2085, Jun. 2011.

[3] B. Farhang-Boroujeny, "OFDM versus filter bank multicarrier," *IEEE Signal Process. Mag.*, vol. 28, no. 3, pp. 92–112, May 2011.

[4] B. Farhang-Boroujeny and C. H. Yuen, "Cosine modulated and offset QAM filter bank multicarrier techniques: A continuous-time prospect," *EURASIP J. Advantage Signal. Process.*, vol. 20, pp. 1–16, Jan. 2010.

[5] M. Schellmann *et al.*, "FBMC-based air interface for 5G mobile: Challenges and proposed solutions," in *Proc. 9th Int. Conf. Cognit. Radio Oriented Wireless Netw. Commun. (CROWNCOM)*, 2014, pp. 102–107.

[6] M. Bellanger *et al.*, *FBMC Physical Layer: A Primer*, PHYDYAS FP7 Project Document, Jan. 2010.

[7] M. Bellanger, "Physical layer for future broadband radio systems," in *Proc. IEEE Radio Wireless Symp. (RWS)*, Jan. 2010, pp. 436–439.

[8] Y. S. Cho, J. Kim, W. Y. Yang, and C. G. Kang, *MIMO-OFDM Wireless Communications With MATLAB*. Hoboken, NJ, USA: Wiley, 2010.

[9] D. Qu, S. Lu, and T. Jiang, "Multi-block joint optimization for the peak-to-average power ratio reduction of FBMC-OQAM signals," *IEEE Trans. Signal Process.*, vol. 61, no. 7, pp. 1605–1613, Apr. 2013.

[10] Z. Kollár and P. Horváth, "PAPR Reduction of FBMC by Clipping and Its Iterative Compensation," *J. Comput. Net. Commun.*, vol. 2012, May 2012, Art. no. 382736.

[11] M. U. Rahim, T. H. Stitz, and M. Renfors, "Analysis of clipping-based PAPR-reduction in multicarrier systems," in *Proc. VTC Spring*, 2009, pp. 1–5.

[12] A. E. Jones, T. A. Wilkinson, and S. Barton, "Block coding scheme for reduction of peak to mean envelope power ratio of multicarrier transmission schemes," *Electron Lett.*, vol. 30, no. 25, pp. 2098–2099, 1994.

[13] J. A. Davis and J. Jedwab, "Peak-to-mean power control and error correction for OFDM transmission using Golay sequences and Reed-Müller codes," *Electron. Lett.*, vol. 33, no. 4, pp. 267–268, Feb. 1997.

[14] V. Tarokh and H. Jafarkhani, "On the computation and reduction of the peak-to-average power ratio in multicarrier communications," *IEEE Trans. Commun.*, vol. 48, no. 1, pp. 37–44, Jan. 2000.

[15] P. Fan and X.-G. Xia, "Block coded modulation for the reduction of the peak-to-average power ratio in OFDM systems," in *Proc. AeroSense*, 1999, pp. 34–43.

[16] X. Wang, T. T. Tjhung, and C. S. Ng, "Reduction of peak-to-average power ratio of OFDM system using a companding technique," *IEEE Trans. Broadcast.*, vol. 45, no. 3, pp. 303–307, Sep. 1999.

[17] T. Jiang and G. Zhu, "Nonlinear companding transform for reducing peak-to-average power ratio of OFDM signals," *IEEE Trans. Broadcast.*, vol. 50, no. 3, pp. 342–346, Sep. 2004.

[18] X. Huang, J. Lu, J. Zheng, K. B. Letaief, and J. Gu, "Companding transform for reduction in peak-to-average power ratio of OFDM signals," *IEEE Trans. Wireless Commun.*, vol. 3, no. 6, pp. 2030–2039, Nov. 2004.
[19] B. S. Krongold and D. L. Jones, "PAR reduction in OFDM via active constellation extension," *IEEE Trans. Broadcast.*, vol. 49, no. 3, pp. 258–268, Sep. 2003.
[20] Z. Yang, H. Fang, and C. Pan, "ACE with frame interleaving scheme to reduce peak-to-average power ratio in OFDM systems," *IEEE Trans. Broadcast.*, vol. 51, no. 4, pp. 571–575, Dec. 2005.
[21] B. S. Krongold and D. L. Jones, "An active-set approach for OFDM PAR reduction via tone reservation," *IEEE Trans. Signal Process.*, vol. 52, no. 2, pp. 495–509, Feb. 2004.
[22] S. H. Müller and J. B. Huber, "OFDM with reduced peak-to-average power ratio by optimum combination of partial transmit sequences," *Electron. Lett.*, vol. 33, no. 5, pp. 368–369, Feb. 1997.
[23] D.-W. Lim, S.-J. Heo, J.-S. No, and H. Chung, "A new PTS OFDM scheme with low complexity for PAPR reduction," *IEEE Trans. Broadcast.*, vol. 52, no. 1, pp. 77–82, Mar. 2006.
[24] Y. Xiao, X. Lei, Q. Wen, and S. Li, "A class of low complexity PTS techniques for PAPR reduction in OFDM systems," *IEEE Signal Process. Lett.*, vol. 14, no. 10, pp. 680–683, Oct. 2007.
[25] J. Hou, J. Ge, and J. Li, "Peak-to-average power ratio reduction of OFDM signals using PTS scheme with low computational complexity," *IEEE Trans. Broadcast.*, vol. 57, no. 1, pp. 143–148, Mar. 2011.
[26] T. Jiang, W. Xiang, P. C. Richardson, J. Guo, and G. Zhu, "PAPR reduction of OFDM signals using partial transmit sequences with low computational complexity," *IEEE Trans. Broadcast.*, vol. 53, no. 3, pp. 719–724, Sep. 2007.
[27] D.-W. Lim, J.-S. No, C.-W. Lim, and H. Chung, "A new SLM OFDM scheme with low complexity for PAPR reduction," *IEEE Signal Process. Lett.*, vol. 12, no. 2, pp. 93–96, Feb. 2005.
[28] C.-L. Wang and Y. Ouyang, "Low-complexity selected mapping schemes for peak-to-average power ratio reduction in OFDM systems," *IEEE Trans. Signal Process.*, vol. 53, no. 12, pp. 4652–4660, Dec. 2005.
[29] Z. Kollár, L. Varga, and K. Czimer, "Clipping-based iterative PAPR-reduction techniques for FBMC," in *Proc. InOWo*, 2012, pp. 1–7.
[30] S. Lu, D. Qu, and Y. He, "Sliding window tone reservation technique for the peak-to-average power ratio reduction of FBMC-OQAM signals," *IEEE Wireless Commun. Lett.*, vol. 1, no. 4, pp. 268–271, Aug. 2012.
[31] R. Gerzaguet, "Comparative study of 5G waveform candidates for below 6 GHz air interface," in *Proc. ETIS Workshop Future Radio Technol., Air Int.*, 2016, pp. 1–9.
[32] S. H. Han and J. H. Lee, "An overview of peak-to-average power ratio reduction techniques for multicarrier transmission," *IEEE Wireless Commun.*, vol. 12, no. 2, pp. 56–65, Apr. 2005.
[33] N. van der Neut *et al.*, "PAPR reduction in FBMC using an ACE-based linear programming optimization," *EURASIP J. Adv. Signal Process.*, vol. 2014, no. 1, pp. 172–192, 2014.
[34] H. Wang, X. Wang, L. Xu, and W. Du, "Hybrid PAPR reduction scheme for FBMC/OQAM systems based on multi data block PTS and TR methods," *IEEE Access*, vol. 4, pp. 4761–4768, 2016.
[35] X. Li and L. J. Cimini, Jr., "Effects of clipping and filtering on the performance of OFDM," in *Proc. VTC*, 1997, pp. 1634–1638.
[36] H. Ochiai and H. Imai, "Performance analysis of deliberately clipped OFDM signals," *IEEE Trans. Commun.*, vol. 50, no. 1, pp. 89–101, Jan. 2002.
[37] H. Ochiai and H. Imai, "Performance of the deliberate clipping with adaptive symbol selection for strictly band-limited OFDM systems," *IEEE J. Sel. Areas Commun.*, vol. 18, no. 11, pp. 2270–2277, Nov. 2000.
[38] D. Gregoratti *et al.*, "Enhanced multicarrier techniques for professional Ad-Hoc and cell-based communications," *ICT-EMPhAtiC Project*, 2015. [Online]. Available: http://www.ict-emphatic.eu/
[39] M. S. Lobo, L. Vandenberghe, S. Boyd, and H. Lebret, "Applications of second-order cone programming," *Linear Algebra Appl.*, vol. 284, nos. 1–3, pp. 193–228, Nov. 1998.
[40] A. Aggarwal and T. H. Meng, "Minimizing the peak-to-average power ratio of OFDM signals using convex optimization," *IEEE Trans. Signal Process.*, vol. 54, no. 8, pp. 3099–3110, Aug. 2006.
[41] T. Jiang and Y. Wu, "An overview: Peak-to-average power ratio reduction techniques for OFDM signals," *IEEE Trans. Broadcast.*, vol. 54, no. 2, pp. 257–268, Jun. 2008.

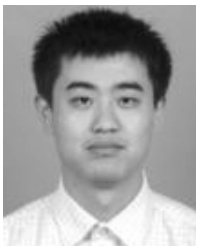

JUNHUI ZHAO (S'00–M'04–SM'09) received the B.S. degree in electrical engineering from the Hefei University of Technology, China, in 1994, the M.S. degree in signal and information systems from Southeast University, China, in 2004, and the Ph.D. degree in communications and electronic systems from Southeast University in 2004. From 1998 to 1999, he was with ZTE Corporation, Nanjing Institute of Engineers. Then, he did his research with the Faculty of Information Technology, Macao University of Science and Technology after being a Visiting Scholar with Yonsei University, South Korea, from 2004 to 2008. In 2008, he joined Beijing Jiaotong University, where he is currently a Professor of the School of Electronics and Information Engineering. His current research interests include wireless and mobile communications and the related application development, which contains 5G mobile communication technology, wireless localization, collaboration and relay communications, channel model, and cognitive radio.

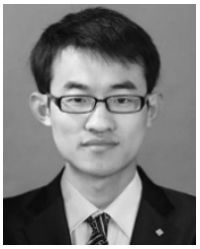

SHANJIN NI received the B.E. degree in communication engineering from China University of Geosciences, Wuhan, China, in 2014. He is currently pursuing the Ph.D. degree with Beijing Jiaotong University, Beijing, China. His current research interests include signal processing, massive MIMO communications, and optimization techniques.

YI GONG (S'99–M'03–SM'07) received the Ph.D. degree in electrical engineering from Hong Kong University of Science and Technology, Hong Kong, in 2002. He joined as a Member of Professional Staff with the Hong Kong Applied Science and Technology Research Institute, Hong Kong. He was employed with Nanyang Technological University, Singapore, where he continues to actively collaborate. He is currently a Professor with South University of Science and Technology of China, Shenzhen, China. His current research interests include cognitive radio, cooperative communications, MIMO, OFDM, and cross-layer design for wireless systems. Since 2006, he has been serving on the editorial board of the IEEE TRANSACTIONS ON WIRELESS COMMUNICATIONS and the IEEE TRANSACTIONS ON VEHICULAR TECHNOLOGY.